JOURNAL OF GEOPHYSICAL RESEARCH, VOL. 107, NO. A10, 1306, doi:10.1029/2002JA009456, 2002

Conjugate observations of traveling convection vortices: The field-aligned current system

D. L. Murr and W. J. Hughes
Center for Space Physics, Boston University, Boston, Massachusetts, USA

A. S. Rodger
Physical Science Division, British Antarctic Survey, Cambridge, United Kingdom

E. Zesta
Department of Atmospheric Sciences, University of California at Los Angeles, Los Angeles, California, USA

H. U. Frey
Space Sciences Laboratory, University of California, Berkeley, California, USA

A. T. Weatherwax[1]
Institute for Physical Science and Technology, University of Maryland, College Park, Maryland, USA

Received 24 April 2002; revised 11 June 2002; accepted 13 June 2002; published 17 October 2002.

[1] Analysis of a single traveling convection vortex (TCV) event that combines magnetometer, auroral imager, and riometer observations from conjugate hemispheres provides a complete view of the field-aligned current (FAC) system associated with the TCV. Conjugate observations clearly show that the TCV is a pair of FACs that flow alternatively out of and then into both ionospheres. Imaging observations at 427.8 nm indicate that the upward FAC region is associated with a narrow arc 50–100 km wide and at least 600 km long. Mapping the imaging observations made in the Southern Hemisphere to the Northern Hemisphere shows excellent collocation of the precipitation with the flow vortex associated with the upward FAC as inferred from a large two-dimensional network of magnetometers. Also consistent with the flows inferred from the magnetometers, the arc is found to be skewed with respect to the direction of motion of the transient. Low-altitude spacecraft passes near the time of the event suggest that the FAC is coincident with, and possibly confined to, a relatively narrow region (less than 3° in latitude) in which 1–10 keV electrons characteristic of the central plasma sheet are present. *INDEX TERMS:* 2409 Ionosphere: Current systems (2708); 2431 Ionosphere: Ionosphere/magnetosphere interactions (2736); 2435 Ionosphere: Ionospheric disturbances; 2463 Ionosphere: Plasma convection; *KEYWORDS:* ionosphere; field-aligned current; traveling convection vortices; conjugate

Citation: Murr, D. L., W. J. Hughes, A. S. Rodger, E. Zesta, H. U. Frey, and A. T. Weatherwax, Conjugate observations of traveling convection vortices: The field-aligned current system, *J. Geophys. Res.*, *107*(A10), 1306, doi:10.1029/2002JA009456, 2002.

1. Introduction

[2] Traveling convection vortices (TCVs) are understood to be the propagating set of vortical ionospheric flows associated with pairs of field-aligned currents (FACs) flowing into and out of the high-latitude ionosphere. This phenomenon was first recognized in high-latitude magnetograms by *Lanzerotti et al.* [1986], *Friis-Christensen et al.* [1988], and *Glassmeier et al.* [1989]. The events were initially believed to be either the ionospheric signature of flux transfer events [*Lanzerotti et al.*, 1986] or a result of FACs connected directly to the magnetopause at the sites of deformations due to solar wind pressure pulses [*Kivelson and Southwood*, 1991]. After their recognition as a distinct phenomenon, statistical studies of TCVs identified their general morphological properties [e.g., *Lanzerotti et al.*, 1991; *Sibeck and Korotova*, 1996; *Zesta et al.*, 2002]. The established TCV characteristics are that they form near noon at latitudes typically near 73° magnetic and propagate antisunward with velocities of 5–10 km/s. They have scale sizes of 1000–3000 km (as determined by magnetometer perturbations) and are observed most frequently a few hours prenoon and postnoon with the majority of events observed in the prenoon sector. The FAC system associated with TCVs maps well inside the magnetosphere, near the central plasma sheet [*Yahnin et al.*, 1997; *Moretto and Yahnin*, 1998], as opposed to earlier studies which linked

[1]Also at Physics Department, Siena College, Loudonville, New York, USA.

0148-0227/02/2002JA009456$09.00

them more directly to processes at the magnetopause. As such, they are an important indicator of how the coupled magnetosphere–ionosphere system responds to transient phenomena.

[3] Due to the availability of observations, many existing studies of TCVs have been based on observations made exclusively in the Northern Hemisphere. TCV studies in the Southern Hemisphere tend to classify events as "magnetic impulse events" (MIEs) as it is difficult to determine whether an event propagates with a limited number of stations. The most comprehensive study of conjugate aspects of these events is the statistical study by *Lanzerotti et al.* [1991] which used an automated analysis to identify MIEs in the Iqaluit (IQA)–South Pole (SPA) conjugate pair of magnetometers. Approximately half the events identified in one hemisphere could be identified at the geomagnetically conjugate magnetometer, within an 8 min window. The study also found MIEs were of similar magnitude in the two hemispheres and that deflections of the vertical component suggested that the same sense of current was flowing into the conjugate locations. A later TCV study by *Lühr et al.* [1993] showed agreement with this pattern by examining extensive observations in the Northern Hemisphere and conjugate single station observations in the Southern Hemisphere. More recently, *Kataoka et al.* [2001] have used extensive observations in both hemispheres to examine an MIE. In the present study we use two-dimensional arrays of magnetometers in conjugate hemispheres together with imaging observations to show conclusively the conjugate nature of a TCV event.

[4] The majority of existing TCV studies have focused on observations from ground magnetometers. Few studies present information about the precipitation region associated with the FAC structures. The earliest and clearest example of these is the study by *Heikkila et al.* [1989]. Using all sky imager (ASI) data from Sondrestrom (STF) (located at 73°N, 42°E in CGM coordinates) they were able to associate the appearance of an arc feature, which propagated across the field of view, with an upward FAC region identified with the Greenland chain of magnetometers. The arc was narrow (50–100 km) and extended across the field of view of the imager. *Mende et al.* [1990] and *Mende et al.* [2001] presented a series of events in which simultaneous 630.0 and 427.8 nm all sky images and magnetic field observations at SPA confirmed the association between MIEs and auroral arcs which formed equatorward of the preexisting dayside cusp aurora (i.e., on closed field lines). *Lühr et al.* [1996] presented a detailed multiinstrument observation of a single TCV in which they also found that the upward FAC region was associated with an arc. They noted that the arc was angled 40° off geomagnetic north (the event was propagating westward) in agreement with magnetometer and VHF radar observations of a skewed convection vortex system. Riometers can also provide information about precipitating particles accompanying transients. *Korotova et al.* [1999] found in a statistical study of 153 MIE events identified in 1 year at SPA, 80% were accompanied by impulsive increases in riometer absorption. As opposed to imagers, riometers can provide information about precipitating particles during sunlit conditions, and thus are useful in conjugate studies. We present here for the first time the relationship between instantaneous maps of the vortical flows associated with a TCV and narrow auroral arcs observed in the conjugate (dark) ionosphere as well as absorption regions observed with conjugate imaging riometers.

[5] We first present ground-based magnetometer observations from the Northern Hemisphere, with data from the MACCS [*Hughes and Engebretson*, 1997], CANOPUS [*Hughes et al.*, 1997], Geological Survey of Canada (GSC), and DMI [*Friis-Christensen et al.*, 1988] networks, to establish the basic morphology and evolution of the event and introduce a new form of presentation of TCV events observed by large two-dimensional magnetometer networks. Similar properties are then derived using magnetometers located in the Southern Hemisphere with data from the British [*Dudeney et al.*, 1997] and U.S. [*Engebretson et al.*, 1997] automatic geophysical observatories (AGOs) and SPA station. After introducing the imaging observations we combine the magnetometer observations from both hemispheres with the 427.8 nm ASI data from SPA to form a composite view of the FAC system. We also examine supporting data sets from low-altitude spacecraft and imaging riometers which confirm many of our conclusions. We conclude by placing the event in the context of existing studies and examine the consequences of the new observations on the current understanding of TCV phenomena.

2. Observations

2.1. Northern Hemisphere Magnetometers

[6] At approximately 1840 UT on 25 July 1997 a large (300 nT at maximum amplitude) transient was observed by the CANOPUS, MACCS, GSC, and Greenland chains of magnetometers. The top eight traces in Figure 1 are a stacked plot of the EW (solid line) and NS (dashed line) components of magnetic variations from several magnetometers located near 75° magnetic latitude, starting near local noon and extending duskward 7 hours in local time (from top to bottom). The time shift of the amplitude peak indicates an eastward propagation of the transient, away from local noon. An analysis of the magnetic perturbation vectors in the horizontal plane shows that the associated equivalent flows are vortical in nature and are an example of a TCV. The bottom trace in Figure 1 is riometer observations of absorption at 38.2 MHz from station IQA. The IQA magnetometer and riometer traces indicate that the largest transient is followed by a second, smaller transient which has an absorption peak at 1848 UT. Several characteristics of the initial TCV, and the FAC system associated with it, can be measured by analyzing the magnetic perturbations from the available two-dimensional network of magnetometer stations. Those characteristics that are critical to this study are the velocity, spatial size and structure, and sense of vorticity of the flow vortices.

[7] Using pairs of these stations near 75° we can estimate the eastward propagation speed of the TCV. Cross correlation analysis was used to align the maxima recorded in the EW component of the variations. The resulting estimated velocity is 5 ± 1 km/s with some indication that this velocity increases from approximately 4 km/s at the beginning of the event to 6 km/s just duskward of 15 MLT (the last available pair of stations). Using stations near 80° the velocity estimate is closer to 3±1 km/s and using pairs of stations near 70° results in an estimate of 8 ± 2 km/s. This change in velocity as a

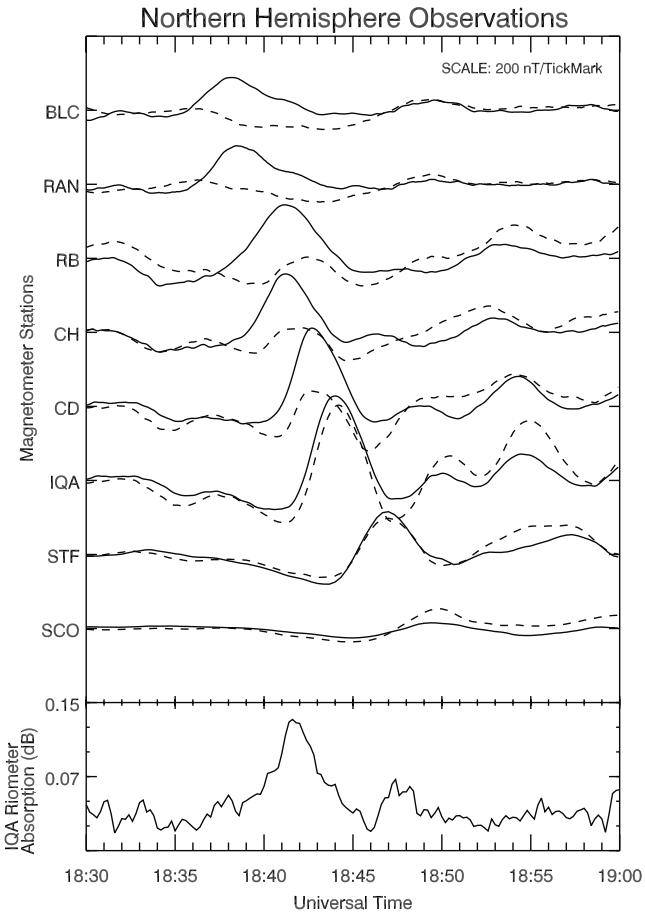

Figure 1. A stacked plot of both EW (solid line) and NS (dashed line) variations for a set of magnetometers in the Northern Hemisphere located near 75° magnetic latitude. The stations are arranged (top to bottom) from west to east, from near local noon to 1700 MLT. The bottom panel shows riometer absorption observed at IQA.

function of latitude is consistent with a constant angular speed of approximately 0.1°/s or about 1 hour in local time every 2 min. However, these estimates are complicated by the fact that the TCV evolves throughout the event, both in amplitude and orientation, and by the uneven spacing of the stations; the estimate near 75° being the most reliable due to both the strong amplitude and the relatively close spacing of the stations. For the stations in Figure 1 the duration of the positive peak is 6 min near the start of the event and is closer to 4.5 min near 15 MLT. Combining this with the estimate of the propagation speeds (including the apparent increase in speed) to calculate the spatial scale of the event results in a constant overall spatial extent of about 1500 km (the distance between the centers of the flow vortices).

[8] Studying the relationship between the perturbations in the two horizontal components reveals information about the sense of vorticity of the transient as well as details about its spatial morphology. As the transient is two dimensional in nature and evolves in time as it propagates, it is rather difficult to summarize all the information contained in the magnetometer perturbations. One way of displaying this information is the use of hodograms. After background values are subtracted the perturbation values of the two horizontal components are plotted against each other tracing out a line or curve over the duration of the event. More convenient to our analysis, this can be done using the components of equivalent overhead flow instead of magnetic perturbation values (a 90° rotation). A brief description of the expected shape of the hodogram curves follows: TCVs are normally thought of as a pair circular flow vortices moving EW in the direction of the line connecting the two centers. In the Northern Hemisphere, if an eastward moving TCV with clockwise and then counterclockwise (or alternatively a counterclockwise followed by clockwise) sense of flow propagated such that the two centers of the vortices passed directly over a magnetometer station, a series of three flow perturbations, all in the NS direction would be seen: first a gradually increasing southward (northward) perturbation as the TCV approached, then a reversal to a northward (southward) perturbation much stronger between the centers of the two vortices, and then a final southward (northward) perturbation as the TCV propagated beyond the station. This pattern can be seen in Figure 1 in the EW component (solid line) of magnetic perturbations, which correspond to NS equivalent flow. The equivalent flow hodogram would trace out a vertical line in the NS flow direction (since there is no EW flow perturbation) that is stronger in one direction. If the centers passed well to the south of a station the flows would be dominated by first an eastward (westward) and then a westward (eastward) flow with smaller NS perturbations as described above. The hodogram would trace out an ellipse with its semimajor axis aligned with the EW flow direction. The smaller NS variations would give it a clear counterclockwise (clockwise) polarization. Finally, if the centers of the TCV passed well to the north of the station the hodogram would be identical but with the opposite polarization.

[9] Figure 2 is a map of magnetometer stations from western Canada to eastern Greenland with hodograms of the inferred flow perturbations plotted over each station. The hodograms were made from 14 min of flow perturbations centered on the amplitude maximum for each station. The location of each station is indicated with a light gray open circle. The starting point of the hodogram is indicated with a solid filled circle and arrows indicate the direction of polarization. The path of the center of the vortices follows the line where the polarization of the hodogram reverses (indicated by larger light-shaded arrows in the figure). As the TCV formed the center was located between stations TAL and BLC at 79.6° and 74.3° near noon MLT. The center of the TCV then shifted equatorward, located south of station CH at 74.8° near 1300 MLT. Subsequently the center of the TCV remained at a constant latitude of approximately 73°, just south of IQA at 1500 MLT (note that there are no stations south of this latitude for the local time sector 13–16) and over stations STF and SCO at 73.2° and 71.6° latitude and 1630 and 1900 MLT, respectively.

[10] The amplitude of the TCV (and thus the hodograms) first increases and then decreases as it propagates across the network of magnetometers. The amplitude of the perturbation linearly increases, reaching its maximum at station IQA at 15 MLT and then decreases until it becomes indistinguishable from other background variations near station SCO (this is also apparent in Figure 1). The rate of increase is approximately 50 nT/h of local time from 1838 (near

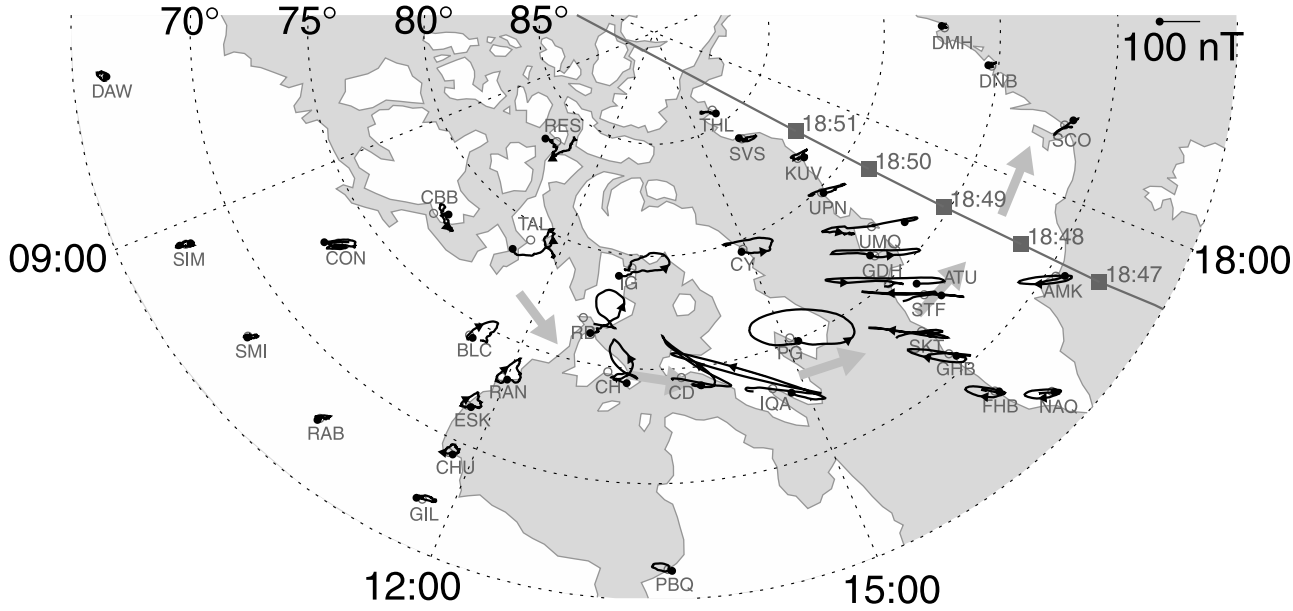

Figure 2. A magnetic local time–magnetic latitude plot with hodograms of equivalent flow, each for 14 min centered on the amplitude maximum observed at each station. Gray open circles show the location of the stations, black filled circles mark the starting point of the hodogram, and arrows show the sense of rotation. Large shaded arrows show the approximate propagation path. The path of a DMSP pass over Greenland is also shown in gray.

station BLC) to 1844 UT (at IQA) and the rate of decrease is approximately 60 nT/h of local time from 1845 to 1850 UT (at station SCO). Along a constant longitude the latitudinal extent for which the perturbation is greater than background variations is slightly less than 15° (∼1600 km). The amplitude variation within this range of latitudes also increases and then decreases nearly linearly. Notice that the amplitude maximum along one longitude does not necessarily correspond to the latitude at which the sign of the polarization reverses. Along the western coast of Greenland the amplitude maximum occurs at station ATU at 74.6° latitude but the polarization reversal occurs at a slightly lower latitude near the station STF at 73.2°.

[11] The linear hodograms where the sign of the polarization reverses (near the center of the TCV) are not aligned at right angles to the direction of TCV motion as would be the case for circular flow vortices. Rather, for this event, the angle between the direction of TCV motion and the major axis of the hodogram varies from approximately 90° at the beginning of the event to near 45° at the time of the maximum amplitude of the event, with the equatorward end tilted into the direction of propagation. This observation indicates that the vortical flows begin nearly circular in nature and then evolve into ellipses tilted into the direction of motion. This evolution of the flow vortices will also introduce errors to our estimate of propagation speed at latitudes significantly far from the center of the vortices. Finally, the magnetic perturbations observed correspond to first a clockwise and then a counterclockwise flow vortex, indicating an upward and then downward FAC pair.

2.2. Southern Hemisphere Magnetometers

[12] Effects of the FACs associated with this TCV were also observed in the Southern Hemisphere. Figure 3 is a stacked plot of magnetic variations from the magnetometers in Antarctica, as well as riometer and photometer observations from SPA, for the same period as plotted in Figure 1 (to aid the comparison with Figure 1 the NS component has been inverted). The locations of the stations in Figure 3 are listed in Table 1. The overall nature of the transient is similar. The station conjugate to IQA (SPA), where the largest amplitude was recorded in the Northern Hemisphere, observes the largest perturbation in the Southern Hemisphere. The stations just to the magnetic north and south of this station, P1 and P2, also show the same decrease in amplitude as a function of latitude that was observed in the north. A significant difference is the timing of the maxima of the stations equatorward of SPA. Although the relative timing between stations P2, A80, and A81 is consistent with the eastward propagation of a TCV, their maxima all occur before that of SPA (even though A80 and A81 are significantly eastward of SPA). This appears to be the effect of a tilted vortex system. In the Northern Hemisphere, the stations along the coast of Greenland show a similar pattern of earlier arrival times the more equatorward the station location. Analysis of the horizontal components of the stations in Figure 3 shows that the center of the TCV passed closest to SPA and that the flows observed at all stations were elliptical in nature, with the equatorward end of the semimajor axis tilted forward into the direction of motion, just as was observed in the Northern Hemisphere. Finally, the sense of the vortical flows observed in the Southern Hemisphere also correspond to first an upward and then a downward FAC.

[13] The network of magnetometers in the Southern Hemisphere is less dense and covers a smaller range of local times than in the north making the estimation of the size and velocity of the TCV more difficult. The only pair of

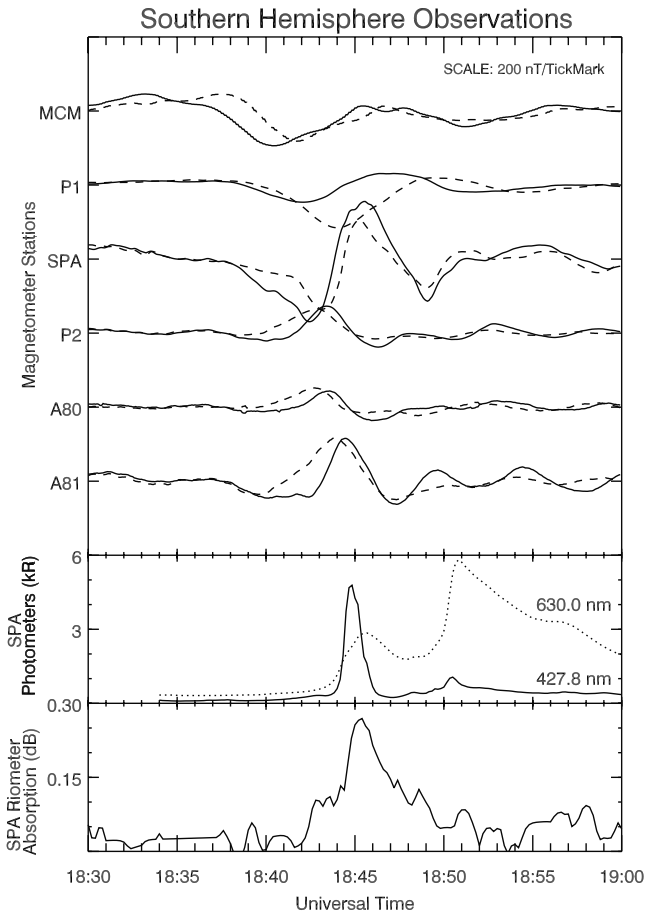

Figure 3. Top panel is a stacked plot of both EW (solid line) and NS (dashed line) variations for magnetometers located in the Southern Hemisphere. The NS component has been inverted (for comparison with Figure 1). The middle panel has traces from the 630.0 and 427.8 nm photometers at SPA. The bottom panel shows riometer absorption at SPA.

stations along a similar latitude available for calculating velocity is the P2 and A81 pair. These stations are near 70° magnetic latitude, nearly 5° equatorward of the TCV center where the most reliable velocity estimate in the Northern Hemisphere was made. Using cross correlation analysis with these two stations, the estimated speed of the transient is 9 ± 1 km/s. This speed is slightly higher to that found for similar (lower) latitudes in the Northern Hemisphere and corresponds to an angular speed of 0.16°/s. Using the duration of the event we find that the distance between the centers of the TCV is 1600 km, similar to that in the Northern Hemisphere.

Table 1. Table of Coordinates of the Southern Hemisphere Magnetometers Used in this Study

Station (Code)	Geographic latitude, longitude	Corrected geomagnetic latitude, longitude
McMurdo (MCM)	77.85°S, 166.67°E	79.94°S, 326.97°E
US AGO P1 (P1)	83.86°S, 129.61°E	80.14°S, 016.87°E
South Pole (SPA)	90.00°S, 000.00°E	74.02°S, 018.35°E
US AGO P2 (P2)	85.67°S, 313.62°E	69.84°S, 019.33°E
BAS AGO 80 (A80)	80.75°S, 339.60°E	66.22°S, 029.39°E
BAS AGO 81 (A81)	81.50°S, 003.00°E	68.54°S, 036.39°E

[14] A subtle feature not readily apparent in comparing Figures 1 and 3 is the presence of a time delay between the two hemispheres. The IQA–SPA pair of stations at similar magnetic latitude and local time observe perturbations similar in shape and amplitude, but the transient is observed 2 min later at SPA. This delay could be due to two effects: either a longitudinal shift of the mapping of field lines such that the field lines map from SPA to somewhere east of IQA (since the TCV is propagating eastward); or the two stations are conjugate (are on close to the same field lines) but there is an actual delay time. Given the velocity of the transient, the first explanation would require an approximately 600–1000 km eastward shift in the mapping of the IQA end of the field line. The second case would imply that the two stations, though located on nearby field lines, are located at different distances from the source region of the FACs. Figure 4 is the meridional view of the field line that connects the IQA and SPA stations as estimated by the 1996 Tsyganenko magnetic field model [*Tsyganenko and Stern*, 1996] using the prevailing solar wind conditions and appropriate date and universal time (1830). During the half hour

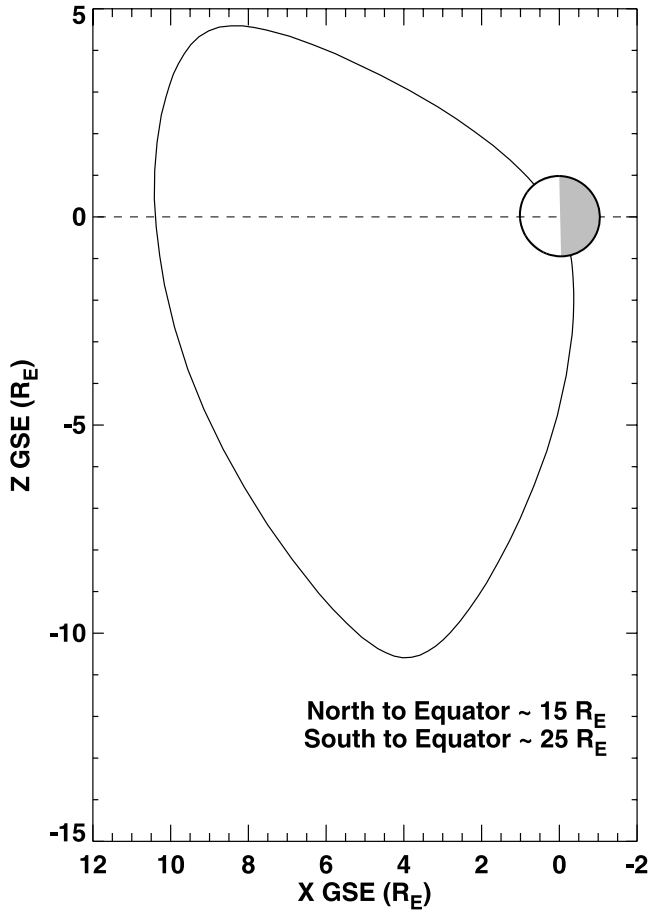

Figure 4. A meridional view of a magnetic field line near local noon and at latitudes near that of stations IQA and SPA at 1830 UT on 25 July 1997 as traced by the Tsyganyenko 1996 magnetic field model.

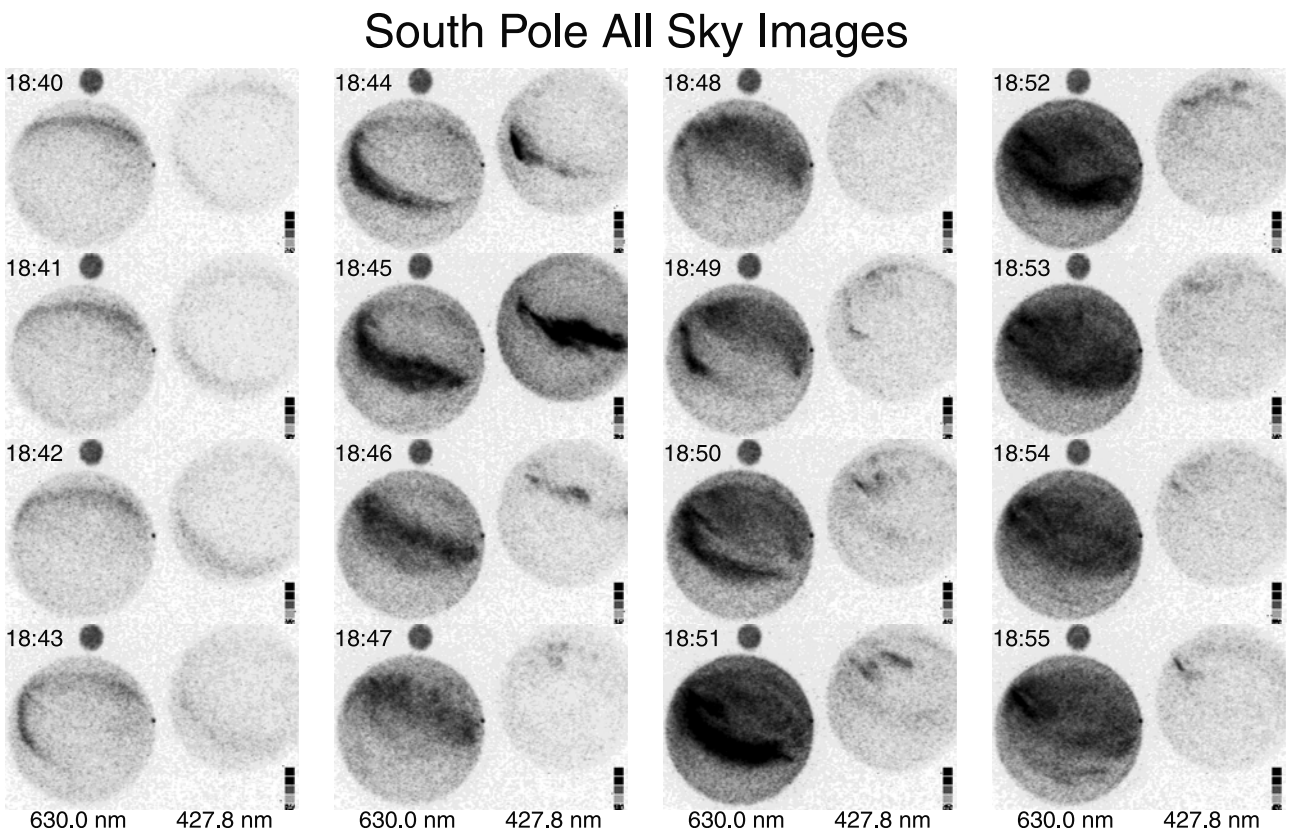

Figure 5. All sky camera images from SPA at 630.0 nm (left side of image) and 427.8 nm (right side of image) every minute for the interval 1840–1855 UT. Geomagnetic south is toward the top of the images and east is to the right.

proceeding the event GEOTAIL observations just upstream of the prenoon bow shock showed the IMF was close to radial with $B_{GSM} \sim$ (2, 0, 1) nT and that the solar wind had a speed of 400 km/s and a density of approximately 15 cm^{-3}. The presence of a trigger in the solar wind during this interval that caused the TCV event will be investigated in a forthcoming paper (E. Zesta et al., in preparation, 2002). Geomagnetic conditions during the event interval were quiet with Kp of 2– during the 3 hour interval containing the event and Kp of 1 for the 3 hour intervals preceding and following the event interval. Tracing field lines at these high latitudes is difficult and the results of the model should only be taken as an indication of the organization of field lines in this region. For our event the model suggests that field lines from SPA map approximately 300 km to the west and north of IQA. This is in the opposite direction of what we would expect for the observed time delay assuming that the time delay is caused by a longitudinal shift of field line mapping. More important, Figure 4 shows that for the date and time of the event the dipole tilt is near its maximum (a necessary condition for obtaining ground-based auroral images at these latitudes on the dayside). The estimated field line lengths from each ionosphere to the ecliptic plane are approximately 15 and 25 R_E. If the FACs were driven by a driver in the ecliptic plane we would expect a propagation delay of ~2 min (assuming a near-equatorial Alfvén speed of 400 km/s, i.e., B $\sim$ 150 nT and n $\sim$ 50 cm^{-3}). While it is likely that the delay is some combination of the two effects, it is clear that the expected longitudinal shift in mapping alone cannot explain the delay.

2.3. Southern Hemisphere Auroral Images

[15] During the interval when the transient was observed in the magnetic recordings at SPA station all sky images were recorded at 630.0 and 427.8 nm once every minute with a 1.8 s exposure. Figure 5 is the set of the raw all sky images covering the interval of the event at SPA. In these raw images the top of the image is in the direction of the southern magnetic pole and right is magnetic east. In both wavelengths a brightening appears in the NW portion of the field of view between 1843 and 1844 UT and propagates eastward reaching the zenith at 1845 and leaving the field of view by 1847. Throughout the interval of 1840–1846, the equatorward edge of the auroral oval can be seen near the top (poleward region) of the 630.0 nm image, indicating that the event occurred on closed field lines (and moreover, that the equatorward edge of the oval remained fixed in location throughout the event). Examining the magnetic perturbation at SPA in Figure 3, the center of the upward field aligned is found between the local minimum at 1843 and local maximum just after 1845 and the center of the downward current passes over SPA between 1847 and 1849. In the upward FAC region we expect to find downward going (precipitating) electrons. Conversely, in the downward FAC region we expect upward going electrons and little or no precipitating electron signatures. Thus, the transient brightening in the images at 1845 (and an absence

of brightening thereafter, keeping in mind that the lifetime of the 630.0 nm emission is about 2 min) recorded at SPA confirms that the magnetic perturbations are caused by an upward FAC followed by an downward FAC. A second brightening in the 630.0 nm images peaks at 1851 UT which corresponds to the second, weaker upward FAC region. The size and shape of this second arc is nearly identical to that at 1845, however the 427.8 nm image at this time shows only a small brightening which is not collocated with the 630.0 nm arc (as was the case at 1845).

[16] Projecting the raw images to an assumed emission height allows estimates of the spatial scale of the precipitation region to be made. The lifetime of the 630.0 nm emission is rather long, typically 110 s. Since the TCV propagates at 5–8 km/s, many of the spatial details of the precipitation region are lost using this emission line. We therefore focus on the 427.8 nm emission as it is a prompt emission (the lifetime is less than a second). Assuming an emission height of 120 km we find that the precipitation region is a narrow linear arc with a width between 50 and 100 km. The length of the arc is difficult to determine with the constraints of the time cadence of the images. The image at 1845 shows the arc extending nearly across the field of view implying a minimum length of approximately 600 km (an upper constraint of the length of the arc cannot be established). Similarly, with 1 min between each image the velocity of the precipitation region is difficult to estimate but the motion of the brightest region in the images at 1844 and 1845 does appear to be consistent with the 5–8 km/s estimate made from the magnetometer observations. Finally, when the projected images are transformed into a geomagnetic coordinate system we find that the arc is aligned along a line with its equatorward end tilted approximately 65° into the propagation direction, the same sense but at a slightly larger angle than was found from magnetometer observations.

[17] The photometers located at SPA station observing 427.8 and 630.0 nm wavelengths integrate over a 60° field of view the sky but have the advantage of sampling once every 10 s. The intensities observed during the event interval are shown at the bottom of Figure 3. They observed a rise from an initial background of less than 0.3 kR at 1843:50 to 4.7 kR at 1844:50 in the 427.8 nm and from 0.5 kR at 1843:30 to 2.8 kR at 1845:30 in the 630.0 nm emissions. There is no emission associated with the downward FAC (upward going electrons), the center of which passes over SPA at about 1847. The second, weaker, upward current shows a much smaller signature in the 427.8 nm wavelength, rising from 0.5 kR before the event at 1849:50 to a maximum of only 1.1 kR at 1850:30. The 630.0 nm wavelength strength rises from an initial 1.9 kR at 1849:00 to a maximum of 5.8 kR at 1850:50 suggesting the precipitating electrons are much softer for the second upward FAC.

2.4. Combined Observations

[18] From the above observations, a synthesized image of the magnetometer measurements in both hemispheres and the all sky images from SPA station can be constructed. This is done in Figure 6 for the interval 1841–1844 UT. The figure was constructed in three steps: First, for visualizing the magnetometer observations in the Northern Hemisphere,

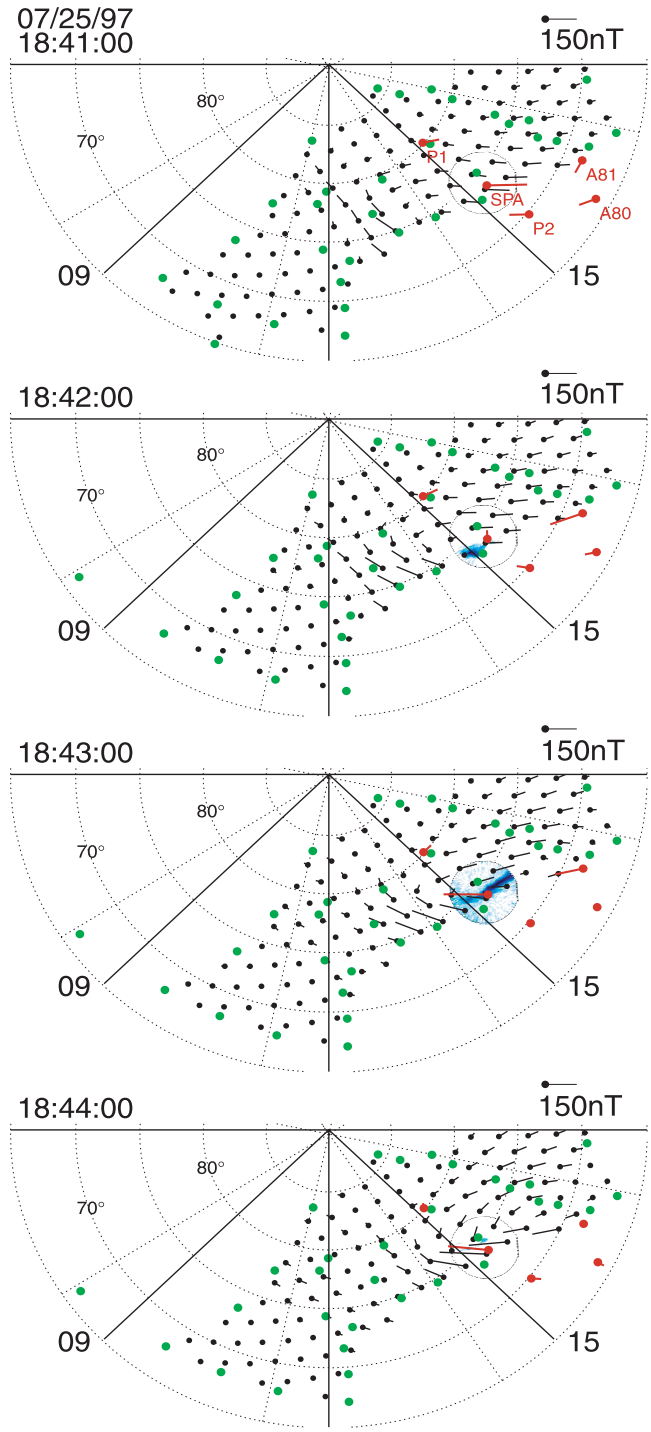

Figure 6. Combined images of equivalent flows derived from magnetometers in both hemispheres and all sky images observed at 427.8 nm at SPA for the interval 1842–1844 UT. Green circles indicate the locations of Northern Hemisphere magnetometer stations. Black vectors (which have filled circles at the base of the vector) indicate the direction of equivalent flow determined from Northern Hemisphere magnetometers. Red vectors indicate equivalent flow direction derived from Southern Hemisphere magnetometers and mapped to the Northern Hemisphere. All Southern Hemisphere data have been time shifted by 2 min.

where we have a large, dense array of magnetometers, we use an interpolation scheme to plot the equivalent flow vectors (described below). Next, the individual equivalent flow vectors from the Southern Hemisphere stations were mapped onto this set of interpolated equivalent flows. Finally, the all sky images from the Southern Hemisphere (after being mapped to an assumed emission height) were mapped onto the combined set of equivalent flows.

[19] The scheme for making the interpolated maps from the Northern Hemisphere magnetometers is rather simple. At each station (locations indicated with larger, green filled circles) quiet level baselines from the magnetically quietest day of the month have been subtracted to obtain magnetic perturbation vectors. These perturbation vectors are rotated 90° into the direction of overhead flow. The individual equivalent flow vectors, recorded at each station, are then linearly interpolated onto an equidistant grid (250 km) to aid in the visualization of the resulting flow field. The flows are interpolated over triangles formed by sets of the three nearest neighboring stations, thus in areas where there are few magnetometers (such as Hudson Bay) flows are interpolated over larger areas resulting in lower spatial resolution. This final point is crucial as there are regions where the distance over which the interpolation is carried out is close to the spatial scale of the TCV. This interpolation scheme is not used for the Southern Hemisphere magnetometers due to the smaller number of stations. The red vectors in Figure 6 are the equivalent flow vectors from the Southern Hemisphere stations mapped to their conjugate locations (using invariant AACGM) in the Northern Hemisphere (with the appropriate rotation) and are labeled with station codes. Finally, the all sky images have also been mapped to the Northern Hemisphere. After projecting the raw image onto an emission height and transformed to a geomagnetic coordinate system, the image is mapped to the Northern Hemisphere rather simply using the invariant AACGM latitude and longitude of each pixel. The field of view of the imager has been denoted with a thin line. For both the magnetic and optical measurements in the Southern Hemisphere we have introduced a 2 min delay when mapping to the Northern Hemisphere, as discussed above.

[20] The set of panels in Figure 6 cover the interval when the TCV passed over the IQA–SPA conjugate pair of stations, as the event reached its maximum amplitude. In the first panel at 1841 (times listed are all in the Northern Hemisphere with the Southern Hemisphere observations delayed by 2 min) the center of the clockwise flows, corresponding to an upward FAC, are centered over 1400 MLT, just west of IQA. Care should be taken in this local time sector as there are no stations to the south of CD and IQA in the Northern Hemisphere. There is reasonable agreement between conjugate flows (black and red vectors) where Southern Hemisphere stations map into a region of interpolated flows in the Northern Hemisphere (such as SPA and P1). Southern Hemisphere stations that do not have close conjugate sites (P2 and A80) or ones which map near the edge of the interpolation region (A81) indicate flows which are consistent with a tilted flow vortex with its equatorward end tilted into the direction of motion. A minute later, as the center of the upward FAC region approaches IQA, auroral emissions are seen near the westward edge of the imager's field of view. By 1843 the center

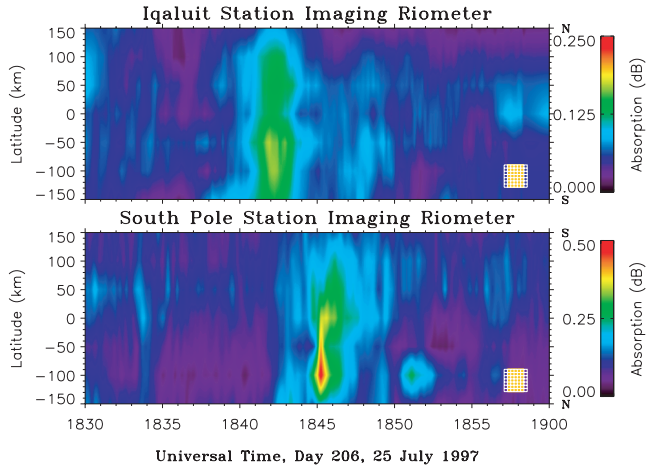

Figure 7. Imaging riometer observations from IQA and SPA stations for 1830–1900 UT. Shown are meridional riograms with latitudinal distance given assuming an absorbing height of 90 km. Note that the intensity scale for SPA is twice that for IQA.

of the upward FAC is located just to the east of the IQA–SPA pair. An auroral arc is aligned with the major axis of the elliptical flow pattern. At 1844 UT the upward FAC region has passed the IQA–SPA pair and has just reached the western coast of Greenland. At this time the precipitation has also left the field of the view of the imager at SPA station.

2.5. Additional Observations

[21] Observations from imaging riometers and low-altitude spacecraft provide supporting evidence for two aspects of the observations described above. Imaging riometers provide an additional confirmation of the conjugate nature of the event and low-altitude spacecraft passes confirm that the FAC occurred on closed filed lines. Imaging riometers observe at 38.2 MHz and are sensitive to electron precipitation in the 10–40 keV range which cause additional ionization and heating in the lower E and D regions. At the time of the event IQA, along with all of the Northern Hemisphere stations, was sunlit and thus the IQA riometer is critical for providing information about precipitating particles. The riometers at IQA and SPA also have the capability of two-dimensional imaging of the precipitation region.

[22] Imaging riometers located at SPA and IQA [*Detrick and Rosenberg*, 1990] observed absorption signatures at the time of the passage of the center of the upward FAC, but not at the time of the downward current. These signatures can be seen in the bottom traces of Figures 1 and 3 which are time series of the maximum absorption observed over the central nine beams of the riometer imaging array. The time series show that the strongest precipitation observed in the Northern Hemisphere, at IQA, occurs at the same time relative to the magnetometer trace as described for the ASI and magnetometer observations at SPA. More simply, the riometer at IQA confirms that the strongest precipitation is collocated with the center of flow vortex associated with the upward FAC. Figure 7 shows riograms from both stations for the period of 1830–

1900 UT. The two panels show meridional slices from the five central beams of the imaging array as a function of time. As was the case with the magnetometer signatures, there is a time delay between the two stations. The time of the maximum absorption at IQA occurs at 1842 UT whereas the time of maximum absorption at SPA occurs at 1845. The amount of absorption observed at SPA is approximately 0.3 dB greater than observed at IQA or about a 7% difference in received power (note that the intensity scales for the two riograms differ by a factor of two). It is important to note that the more energetic precipitating electrons responsible for the riometer signal account for a small fraction (possibly less that 1%) of the total energy flux of the precipitating electrons in the upward FAC region and therefore the riometer signals may provide information about more energetic acceleration processes within the FAC but are not necessarily good indicators of the overall current structure. Additionally, a much weaker absorption was also observed with a broad-beam riometer at STF where the magnetic signature was also smaller. Two-dimensional images of the absorption at SPA (not shown) indicate a region of enhanced absorption approximately 100 km in width and more than 200 km in length (the field of view of the imaging riometer is 200 km on a side) with the equatorward edge angled 60° into the direction of motion, very similar to the 427.8 nm all sky imaging observations. Finally, a second region of much less intense absorption was observed at 1848 at IQA and 1851 at SPA (the time delay between the hemispheres is the same as the prior absorptions). These absorptions correspond to the upward FAC of a second, weaker, TCV pair also observed in the magnetometer data. For both upward FACs the region of maximum absorption is observed to be just equatorward of IQA and SPA, suggesting that both stations are slightly poleward of the most intense precipitation region. The mapping of field lines using the Tsyganyenko 1996 model suggested that SPA would map 200–300 km poleward of IQA, these observations suggest that the two stations are located much closer in latitude.

[23] Near the time of the event the DMSP low-altitude spacecraft passed near the 18 magnetic local time sector in the Northern Hemisphere (over Greenland). The track of the DMSP F13 is marked in Figure 2. The precipitating electron and ion data observed by the F13 satellite are plotted in Figure 8. Precipitating electrons in the hundreds of eV are present throughout the interval of 1848:00–1850:50, or magnetic latitudes of 71.7° to 82°. Imbedded in the lower energy electrons is a band of 1–10 keV electrons observed from 1848:20 to 1849:10, or latitudes of about 73° to 76° magnetic. From the magnetometer observations on the western coast of Greenland, the center of the TCV is located at approximately 73.5°, near the equatorward edge of the 1–10 keV electron region. DMSP observes a small arc at 1849:00 (75.4° magnetic latitude). The station nearest this latitude on the west coast of Greenland is ATU (see Figure 2). Propagating the flow vortex system from the observations at ATU to the location of DMSP at 1849 (at a speed of 6 km/s) we find that the observed arc coincides exactly with the upward FAC region. DMSP observes the arc over approximately 0.1° in magnetic latitude or about 10 km (essentially the spatial resolution of DMSP) which is of the same order of the arc width observed by the ASIs.

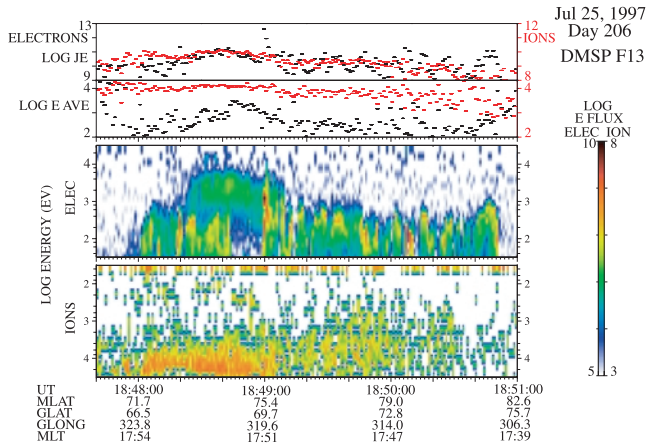

Figure 8. DMSP precipitating particle observations during an overpass of Greenland (the satellite path is marked in Figure 2) near the time of the event. The top two panels show the energy flux and average energy of ions and electrons. The next two panels are time–energy spectrograms of electrons and ions.

3. Discussion

3.1. Morphology and Evolution

[24] In many respects the event presented here possesses typical TCV morphological properties. Its spatial size of 1600 km, its velocity of 5 ± 1 km/s, and maximum amplitude of 300 nT (as determined in the Northern Hemisphere) are within the range of those presented by previous authors. The TCV is clearly an upward then downward pair of FACs propagating eastward, away from local noon followed by a smaller pair of upward then downward currents. The vortices also appear to be skewed with respect to the direction of motion as reported for previous event studies. Using the existing large two-dimensional networks of magnetometers we are able to determine how these properties evolve as the event progresses.

[25] A few event studies of TCVs have fully utilized the two-dimensional networks of high-latitude magnetometers that are now available [*Lühr and Blawert*, 1994; *Moretto et al.*, 1997; *Zesta et al.*, 1999; *Kataoka et al.*, 2001]. In this study, with the network of magnetometers in the Northern Hemisphere, we have shown the evolution characteristics of the transient. The amplitude linearly increases at a rate of 50 nT/h of local time from near noon to 15 MLT and then linearly decreases at a rate of 60 nT/h until it is indistinguishable from other variations (though remaining within the field of view). Similar amplitude evolution has been reported in the global event studies by *Moretto et al.* [1997] and *Zesta et al.* [1999] and it is now clear that the TCV event occurrence maxima near 9 and 15 MLT that has been found in statistical studies [e.g., *Lanzerotti et al.*, 1991; *Sibeck et al.*, 1998; *Zesta et al.*, 2002] can be explained in terms of an amplitude threshold in selection criteria. The statistical studies also tend to show a higher occurrence rate for events near 9 MLT compared to 15 MLT. *Sibeck and Korotova* [1996], using the statistical conductivity maps of

Hardy et al. [1987], suggested that this dawn–dusk asymmetry may be due to the asymmetry in background Hall conductivity. Although this may explain dawn–dusk asymmetry in the occurrence statistics (by raising and lowering the amplitude threshold) it does not explain the evolution of the strength of an individual event.

[26] For the current study, the overall size of the system appears to remain fixed as the TCV evolves. The shape, however, does appear to evolve. As seen in Figure 2, hodograms from stations near the onset of the event (near noon) observe nearly circular polarization. By approximately 13–14 MLT the hodograms begin to show a skewing or tilt that has been previously reported [e.g., *Friis-Christensen et al.*, 1988; *Friis-Christensen*, 1990; *Lühr and Blawert*, 1994; *Moretto et al.*, 1997]. The angle appears to reach its maximum value of $\sim 45^\circ$ by 15 MLT and remains approximately constant throughout the subsequent observations. The original explanation by *Friis-Christensen* [1990] is based on the mapping of the field lines involved in a TCV. At that time it was believed that the high-latitude region of the TCV mapped along highly draped field lines to the boundary layer while the lower-latitude region of the TCV mapped along nearly dipolar field lines. If this were the case, a radial structure in the magnetosphere would map to a tilted structure in the ionosphere. We have used the Tsyganenko 1996 magnetic field model to map radial magnetospheric structures to the ionosphere for the field lines appropriate to this event (which map to 7–8 R_E in the ecliptic plane). We find that the tilting from this mapping only explains about half of the amount of tilting observed. We therefore propose that the skewed flow vortices are not solely due to mapping but are possibly a reflection of the driving magnetospheric flows as well.

[27] The path of the center of the vortices in this event is traced over 6 hours of local time. The TCV forms (in the field of view of the magnetometers) near noon at $76^\circ \pm 2^\circ$ latitude; propagating eastward, the center passes through $73^\circ \pm 1^\circ$ at 15 MLT and $72^\circ \pm 1^\circ$ at 18 MLT at which point its amplitude has diminished to the level of other, unrelated variations. This slight equatorward shift of the TCV center has been reported by *Lühr and Blawert* [1994], *Moretto et al.* [1997], and *Zesta et al.* [1999]. By examining precipitating particles observed by low-altitude spacecraft near the time of TCV events, the studies of *Yahnin et al.* [1997] and *Moretto and Yahnin* [1998] have shown clearly that the center of TCV events occur within regions of central plasma sheet-like (CPS) precipitation close to the CPS/BPS boundary. Furthermore, the statistical study of precipitating particles observed by the low-altitude DSMP spacecraft by *Newell and Meng* [1992] shows that the dayside location of the CPS/BPS boundary is centered near 75° close to noon and decreases to 70° at the dawn and dusk flanks. It is therefore likely that the path of the TCV follows the latitudinal variation of the mapped CPS location or the CPS/BPS boundary. Additionally, DMSP observations presented here show definitively that the precipitating electrons associated with the upward FAC are located within the plasma sheet-like precipitation region.

3.2. Conjugate Aspects

[28] Although there does not exist an equivalently large two-dimensional network of magnetometers in the Southern Hemisphere, there is a sufficient number to examine the general morphological properties of the TCV in the conjugate hemisphere. The maximum amplitude of the TCV is similar (300 nT) at conjugate locations. The propagation speed of 0.16°/s in the Southern Hemisphere is also similar to that found in the Northern Hemisphere. The overall spatial scale of the event is also similar, 1500 km in the south compared to 1600 km in the north. For all these measurements the greater number of observations in the Northern Hemisphere tends to lead to a more accurate estimation and so differences between the conjugate values may reflect the lesser accuracy of the measurements in the Southern Hemisphere. Therefore we do not regard these differences as geophysically significant. This is the first time these parameters have been accurately established simultaneously in both hemispheres and it is clear that the TCV in the present study (and likely in general) is a conjugate phenomenon which occurs on closed field lines.

[29] As suggested by the statistical study of a single conjugate pair of stations by *Lanzerotti et al.* [1991], the TCV in this study has been shown conclusively to be a pair of FACs, first directed out of and then into both hemispheres. This was established not only by the sense of the convection vortices inferred from the magnetometers in the separate hemispheres but also by the conjugate imaging riometer observations. The amplitude of the magnetic perturbations was similar in the two hemispheres. Modeling studies by *Zhu et al.* [1999] have predicted that for a voltage driven precipitation source, large differences in amplitude and structure will be observed by magnetometers in sunlit and dark conditions. Their model suggests that the amplitude of magnetometer perturbations will be nearly three times larger in an ionosphere with a background conductivity of 7 mho compared to that with a background of 2 mho. We did not observe such a difference in the sunlit and dark ionospheres for this event, the amplitudes were nearly the same (as was found on average in the *Lanzerotti et al.* [1991] conjugate study). This suggests that the assumption of a voltage driver in the model is incorrect and that TCVs are driven by a current source in the magnetosphere (with further evidence presented below).

3.3. Precipitation and Current Structure

[30] MIEs and in some cases TCVs have been shown to be related to auroral arcs observed at either 630.0, 557.7, or 427.8 nm with all sky cameras [*Heikkila et al.*, 1989; *Mende et al.*, 1990, 2001; *Lühr et al.*, 1996; *Kataoka et al.*, 2001]. We have shown the direct relationship between the vortical flows inferred from ground-based magnetometers and a narrow auroral arc observed at 427.8 and 630.0 nm in the conjugate hemisphere. The arc has a width of 50–100 km and a length of at least 600 km. The arc is found to be collocated with the flow vortex (determined from magnetometer observations) associated with the upward FAC. The arc is tilted at an angle with respect to its direction of motion in a similar way, but by a slightly larger amount than the flow vortex observed by the magnetometers. This is the first time that the spatial structure of the auroral precipitation and the flow vortices has been directly related. All existing theoretical models of the TCV current system [e.g., *Glassmeier and Heppner*, 1992; *Lühr et al.*, 1996] use a simple pair of line currents. The observations in this study suggest

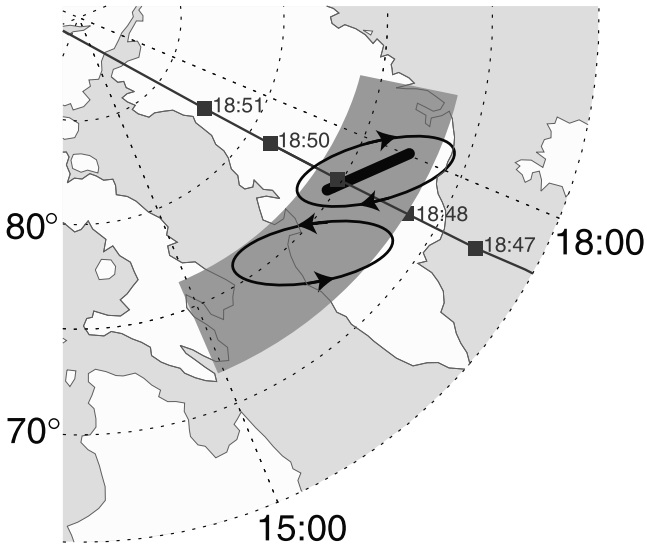

Figure 9. A schematic cartoon summarizing the observations of the FAC system in this study by superposing the magnetometer observations from the Northern Hemisphere, the all sky imaging observations from the Southern Hemisphere, and the low-altitude spacecraft observations.

that sheet currents of finite length and skewed in the direction of motion may be a more realistic model.

[31] The cartoon in Figure 9 summarizes the observations of the FAC system in this study by superposing the magnetometer, all sky imaging, and low-altitude spacecraft observations of the event. The ellipses represent the pair of flow vortices observed by the Northern Hemisphere magnetometers, indicating their tilted configuration and sense of flow direction. The tilted black bar represents the precipitation region observed by the ASIs in the Southern Hemisphere. Both of these aspects of the FAC system have been propagated eastward at 5 km/s from their time of observation, 1842 UT, near the IQA–SPA conjugate pair. The figure also shows the path of the DMSP orbit from 1847 to 1851 UT. The gray-shaded region from near 72° to 76° indicates the region where DMSP observed plasma sheet-like precipitation (the shading has been extended to the east and west along constant latitudes). Imbedded within this region DMSP observed a narrow arc at 1849 UT, just where it should have crossed the tilted arc feature observed by the all sky cameras, had the arc remained similar in size and shape and propagated 5 km/s eastward.

[32] Rough estimates of the current strength can be made from the photometric observations. To within an order of magnitude the precipitating energy flux and characteristic energy of the precipitating electrons can be deduced from the 630.0 and 427.8 nm observations [see *Robinson and Vondrak*, 1994, and references therein]. Studies have found that the 427.8 nm emission is proportional to the total precipitating energy flux with a proportionality constant of 200–300 R/erg [*Steele and McEwen*, 1990]. Thus, for the first upward FAC the incident energy flux was of order 15–25 erg/cm^2 s or about 2×10^{12} J/m^2 s. An estimate of the characteristic energy of the precipitating electrons can be made by evaluating the ratio of the 630.0 and 427.8 nm emissions [*Steele and McEwen*, 1990]. The ratio at their peak values was about 0.6, indicating a characteristic energy of 2 ± 1 keV. Combining the characteristic energy with the incident energy flux yields a current density of the order 10 μA/m^2, similar to the previous estimates of *Lanzerotti et al.* [1991] and *Lühr and Blawert* [1994]. Furthermore, if we assume an arc length of 600 km and a width of 50 km, then the total current (within the field of view of the imagers) is about 300 kA. This is the most direct estimate of the current carried in a TCV event to date and it has no assumptions about the FAC system geometry as previous authors have had to make [*Lanzerotti et al.*, 1991; *Lühr and Blawert*, 1994]. Finally, we note that the precipitating energy flux of electrons observed in the Northern Hemisphere by the DMSP spacecraft (top panel of Figure 8 at 1849 UT) is of the same order as observed in the Southern Hemisphere and that the characteristic energy was about 2 keV (see Figure 8). This suggests that the energetic characteristics of the upward FAC region in the two hemispheres are fairly similar even though one hemisphere is sunlit and one dark. However, the DMSP observations occur about 4 min after the observations in the Southern Hemisphere, as the TCV has begun to diminish in intensity (as observed by the magnetometers).

[33] The nature and structure of the precipitation region associated with an individual TCV/MIE event may be an important discriminator of the various types of TCVs and possibly of their drivers. The MIE event examined by *Weatherwax et al.* [1999] had a much different auroral signature than the event described here as well as the auroral signatures identified by *Mende et al.* [1990, 2001]. Rather than a narrow arc, the event in the work of *Weatherwax et al.* [1999] was characterized by the filling of the entire field of view of the all sky camera at 427.8 nm. That event was associated with a discontinuity in the interplanetary magnetic field of the type which leads to the formation of a hot flow anomaly (HFA) at the bow shock and magnetopause [*Sibeck et al.*, 1998; *Sitar et al.*, 1998]. The conclusion from these studies was that hot flow anomalies may be the drivers of a significant number of MIE/TCV events. However, we find that the 427.8 nm all sky camera observations indicate that the *Weatherwax et al.* [1999] event is unlike the event presented here as well as the majority of events presented in the literature which include all sky camera observations. Thus, observing the intensity and structure of the precipitation associated with MIE/TCV events may be critical in understanding the magnetospheric driver of the phenomenon.

3.4. Implications for a Magnetospheric Driver

[34] Many questions remain regarding the driver and source region of the FAC system that produces TCVs. Early models suggested that the currents were driven at indentations along the surface of the magnetopause [*Kivelson and Southwood*, 1991], providing a direct connection between magnetopause processes and the high-latitude ionosphere. Recently it has been shown that TCVs occur on closed field lines well within the magnetosphere [*Moretto and Yahnin*, 1998]. Hence, regardless of the ultimate driver of the transient current system (in the solar wind or magnetosheath), a new consideration is where and how the transient is coupled, or where the maximum coupling occurs, within the magnetosphere.

[35] The organization of the currents flowing (on closed field lines) alternatively out of and then into both ionospheres implies, as was pointed out in the *Lanzerotti et al.* [1991] study, that the flux tubes have been twisted somewhere along the field line, driving Alfvén waves carrying current into both hemispheres. Any significant differences in the length of the field line (or integrated Alfvén velocities) from the location of the driver to the two ionospheres will cause the waves to reach the two ionospheres at different times. Thus, the location of the driver along the field line may be deduced from analyzing any delays observed between the two hemispheres. The event considered in this paper occurred on 25 July at a universal time when the dipole tilt was at 29° or 85% of its maximum value. The difference in the field line lengths from the ecliptic to each hemisphere was estimated to be between 5 and 10 R_E by tracing field lines with the Tsyganenko 1996 magnetic field model. The observed delay was approximately 100 s, suggesting a constant Alfvén speed in the range of 300–600 km/s. The observed delay between the Northern and Southern Hemispheres is thus consistent with a driver located near the ecliptic (i.e., the plane that contains the solar wind vector). This is a rather simplistic argument as the Alfvén speed may vary differently along the field line for the two hemispheres depending on the field geometry. The significant difference in conductivities between the hemispheres (which will be present for a large dipole tilt) may also control coupling timescales and thus any time delay between the conjugate ionospheres.

[36] Properties of the spatial structure of the driver region can be estimated from the spatial structure of the current system observed in the ionosphere. We found the region of the most intense precipitation to be a narrow feature, approximately 50–100 km wide and over 600 km long with its equatorward edge angled approximately 65° into the direction of motion of the TCV. This observation is in good agreement with the spatial structure estimate from the two-dimensional network of magnetometers in the Northern Hemisphere. Using the Tsyganenko 1996 model to map the extent of the arc to the ecliptic plane in the magnetosphere results in a region that has an azimuthal extent of at least 3–4 R_E and a radial extent of about 1 R_E. If we expect the FACs to be driven by a twisting of field lines or flow shears in this region of the magnetosphere then the elongated nature of the region will tend to produce strong azimuthal flows (as opposed to circular flows) in the magnetosphere, as was observed by *Moretto et al.* [2002]. The tilted nature of the arc, mapped to the magnetosphere, implies that the leading edge of the driver will be slightly inward of the trailing edge. Again, this is a fairly simple argument and it is likely that we cannot attribute all features of the precipitation region to a direct mapping of the driving region. Some properties of the precipitation pattern may be determined by local conductivities or possibly an intermediate acceleration region.

[37] The large two-dimensional network of magnetometers in the Northern Hemisphere allows the path of the TCV in the ionosphere to be well determined. We can use this information to estimate the motion of the driving flow shears in the magnetosphere. The initial detection of the event (just as it becomes distinguishable from background variations) occurs of field lines near local noon which map very near to the magnetopause. Subsequently the TCV moves slightly equatorward as it propagates eastward. Similar patterns of motion have been described in the global studies of *Moretto et al.* [1997] and *Zesta et al.* [1999]. The roughly 3° equatorward motion translates to about 4 R_E inward motion in the magnetosphere. The TCV then travels at a nearly constant magnetic latitude of 73° which maps to an equatorial radial distance of 7–8 R_E. DMSP measurements at 18 MLT near the time of the event show plasma sheet like precipitation from 73° to 76° magnetic latitude, mapping the center of the TCV to the inner edge of this region. The angular speed of the TCV in the ionosphere was found to be about an hour in local time every 2 min. At 7–8 R_E this translates to an azimuthal propagation of the driver region of 150 km/s or roughly magnetosheath speeds.

[38] If we follow the assumption that the currents are driven by the twisting of flux tubes, then the amplitude of the TCV in the ionosphere will be related to the amount of twisting or the flow shears causing the twisting in the magnetosphere and their evolution throughout the event. It may be that the amplitude profile (in latitude and longitude) is defined predominately by magnetospheric properties. The amplitude maximizes near 15 MLT, presumably mapping to the region of strongest shear. As the transient passes beyond 15 MLT it enters the flank region of the magnetosphere which flares, the flux tubes expand and the amount of shear decreases.

[39] In summary, the combined ionospheric observations made during this event imply several characteristics of the magnetospheric driver: The currents are likely to be driven by a twisting or flow shear across magnetic flux tubes in the ecliptic plane of the magnetosphere. The flow shears occur over an azimuthally extend region of 3–4 R_E with a radial thickness of approximately 1 R_E. This region is located 1–2 R_E beyond geosynchronous orbit near the central plasma sheet and propagates through the magnetosphere at a speed of 150 km/s. The amplitude and thus the strength of the flow shear increases until reaching its maximum near 15 MLT and decreases thereafter.

4. Conclusion

[40] By combining observations from large networks of magnetometers with auroral imaging we have provided the most complete view of the FAC system associated with a TCV event. The conjugate observations have clearly shown that the system consists of a pair of FACs directed alternatively out of and into the northern and southern ionospheres. Auroral images show that the upward current region (downward going electrons) has the form of a narrow arc 50–100 km wide and more than 600 km long. The arc and the associated equivalent flows are skewed with the equatorward edge tilted into the direction of motion. Low-altitude spacecraft observations show that the system of currents is confined to a narrow region (approximately 3° in latitude) in which 1–10 keV electrons characteristic of the central plasma sheet are present. The current density of the FAC system was found to be approximately 10 $\mu A/m^2$ and characteristic energies of the precipitating electrons were observed to be 1–2 keV in both the sunlit and dark ionospheres. These observations are consistent with a magnetospheric driver in which a region of flow shear exists 1–2 R_E

beyond geosynchronous orbit, within the central plasma sheet, about 1 R_E in width and extending at least 3–4 R_E in azimuth.

[41] **Acknowledgments.** The MACCS magnetometer array is supported through National Science Foundation grants ATM9704766 at Boston University and ATM0000339 at Augsburg College. Additional support for this work was provided by NSF grant ATM0000950 at Boston University. The CANOPUS instrument array, operated by the Canadian Space Agency, provided data used in this study. Natural Resources Canada operates the Geological Survey of Canada magnetometer observatories. The Danish Meteorological Institute operates the Greenland coastal magnetometer stations and data were provided by J. Watermann. The University of Maryland receives support under grants OPP-9818176 and OPP-0003881. We thank Louis Lanzerotti of Lucent Technologies for use of South Pole magnetometer data. We thank Mai Lam of BAS for her help with data analysis for this paper. Finally, we wish to acknowledge the International Space Science Institute in Bern, Switzerland, for supporting and hosting the TCV workshop in the summer of 2000 where this work was initiated.

References

Detrick, D. L., and T. J. Rosenberg, A phased-array radiowave imager for studies of cosmic noise absorption, *Radio Sci.*, *25*, 325, 1990.

Dudeney, J. R., R. B. Horne, M. J. Jarvis, R. I. Kressman, A. S. Rodger, and A. J. Smith, British Antarctic Survey's ground-based activities complementary to satellite missions such as Cluster, in *Satellite-Ground Based Coordination Sourcebook, ESA Publ. SP-1198*, pp. 101–110, edited by M. Lockwood et al., ESA, Noordwijk, Netherlands, 1997.

Engebretson, M. J., et al., The United States Automatic Geophysical Observatory (AGO) program in Antarctica, in *Satellite-Ground Based Coordination Sourcebook, ESA Publ. SP-1198*, pp. 65–100, edited by M. Lockwood et al., ESA, Noordwijk, Netherlands, 1997.

Friis-Christensen, E., Terrestrial ionospheric signatures of field-aligned currents, in *Physics of Magnetic Flux Ropes, Geophys. Monogr. Ser.*, vol. 58, edited by C. T. Russell et al., p. 605, AGU, Washington, D. C., 1990.

Friis-Christensen, E., M. A. McHenry, C. R. Clauer, and S. Vennerstrom, Ionospheric traveling convection vortices observed near the polar cleft: A triggered response to changes in the solar wind, *Geophys. Res. Lett.*, *15*, 253, 1988.

Glassmeier, K. H., and C. Heppner, Traveling magnetospheric convection twin-vortices: Another case study, global characteristics, and a model, *J. Geophys. Res.*, *97*, 3977, 1992.

Glassmeier, K. H., M. Honisch, and J. Untiedt, Ground-based and satellite observations of traveling magnetospheric convection twin vortices, *J. Geophys. Res.*, *94*, 2520, 1989.

Hardy, D. A., M. S. Gussenhoven, R. Raistrick, and W. J. McNeil, Statistical and functional representations of the pattern of auroral energy flux, number flux, and conductivity, *J. Geophys. Res.*, *92*, 12,275, 1987.

Heikkila, W. J., T. S. Jorgensen, L. J. Lanzerotti, and C. G. MacLennan, A transient auroral event on the dayside, *J. Geophys. Res.*, *94*, 15,291, 1989.

Hughes, W. J., and M. J. Engebretson, MACCS: Magnetometer array for cusp and cleft studies, in *Satellite-Ground Based Coordination Sourcebook, ESA Publ. SP-1198*, pp. 119–130, edited by M. Lockwood et al., ESA, Noordwijk, Netherlands, 1997.

Hughes, T. J., F. Creutzberg, D. R. McDiarmid, D. D. Wallis, G. Rostoker, J. C. Samson, and L. L. Cogger, The CANOPUS ground-based auroral instrument array, in *Satellite-Ground Based Coordination Sourcebook, ESA Publ. SP-1198*, pp. 131–144, edited by M. Lockwood et al., ESA, Noordwijk, Netherlands, 1997.

Kataoka, R., H. Fukunishi, L. J. Lanzerotti, C. G. Maclennan, H. U. Frey, S. B. Mende, J. H. Doolittle, T. J. Rosenberg, and A. T. Weatherwax, Magnetic impulse event: A detailed case study of extended ground and space observations, *J. Geophys. Res.*, *106*, 25,873, 2001.

Kivelson, M. G., and D. J. Southwood, Ionospheric traveling vortex generation by solar wind buffeting of the magnetopause, *J. Geophys. Res.*, *96*, 1661, 1991.

Korotova, G. I., T. J. Rosenberg, L. J. Lanzerotti, and A. T. Weatherwax, Cosmic noise absorption at South Pole during magnetic impulse events, *J. Geophys. Res.*, *104*, 10,327, 1999.

Lanzerotti, L. J., L. C. Lee, C. G. Maclennan, A. Wolfe, and L. V. Medford, Possible evidence of flux transfer events in the polar ionosphere, *Geophys. Res. Lett.*, *13*, 1089, 1986.

Lanzerotti, L. J., R. M. Konik, A. Wolfe, D. Venkatesan, and C. G. MacLennan, Cusp latitude magnetic impulsive events, 1, Occurrence statistics, *J. Geophys. Res.*, *96*, 14, 1991.

Lühr, H., and W. Blawert, Ground signatures of travelling convection vortices, in *Solar Wind Sources of Magnetospheric ULF Waves, Geophys. Monogr. Ser.*, vol. 81, edited by M. J. Engebretson et al., p. 231, AGU, Washington, D. C., 1994.

Lühr, H., W. Blawert, and H. Todd, The ionospheric plasma flow and current patterns of travelling convection vortices: A case study, *J. Atmos. Terr. Phys.*, *55*, 1717, 1993.

Lühr, H., M. Lockwood, P. E. Sandholt, T. L. Hansen, and T. Moretto, Multi-instrument ground-based observations of a travelling convection vortices event, *Ann. Geophys.*, *14*, 162, 1996.

Mende, S. B., R. L. Rairden, L. J. Lanzerotti, and C. G. MacLennan, Magnetic impulses and associated optical signatures in the dayside aurora, *Geophys. Res. Lett.*, *17*, 131, 1990.

Mende, S. B., H. U. Frey, J. H. Doolittle, L. J. Lanzerotti, and C. G. MacLennan, Dayside optical and magnetic correlation events, *J. Geophys. Res.*, *106*, 24,637, 2001.

Moretto, T., and A. Yahnin, Mapping travelling convection vortex events with respect to energetic particle boundaries, *Ann. Geophys.*, *16*, 891, 1998.

Moretto, T., E. Friis-Christensen, H. Lühr, and E. Zesta, Global perspective of ionospheric traveling convection vortices: Case studies of two Geospace Environment Modeling events, *J. Geophys. Res.*, *102*, 11,597, 1997.

Moretto, T., M. Hesse, A. Yahnin, A. Ieda, D. Murr, and J. F. Watermann, Magnetospheric signature of an ionospheric travelling convection vortex event, *J. Geophys. Res.*, *107*, 1072, doi:10.1029/2001JA000049, 2002.

Newell, P. T., and C.-I. Meng, Mapping the dayside ionosphere to the magnetosphere according to particle precipitation characteristics, *Geophys. Res. Lett.*, *19*, 609, 1992.

Robinson, R. M., and R. R. Vondrak, Validation of techniques for space based remote sensing of auroral precipitation and its ionospheric effects, *Space Sci. Rev.*, *69*, 331, 1994.

Sibeck, D. G., and G. I. Korotova, Occurrence patterns for transient magnetic field signatures at high latitudes, *J. Geophys. Res.*, *101*, 13,414, 1996.

Sibeck, D. G., N. L. Borodkova, G. N. Zastenker, S. A. Romanov, and J. A. Sauvaud, Gross deformation of the dayside magnetopause, *Geophys. Res. Lett.*, *25*, 453, 1998.

Sitar, R. J., J. B. Baker, C. R. Clauer, A. J. Ridley, J. A. Cumnock, V. O. Papitashvili, J. Spann, M. J. Brittnacher, and G. K. Parks, Multi-instrument analysis of the ionospheric signatures of a hot flow anomaly occurring on July 24, 1996, *J. Geophys. Res.*, *103*, 23,357, 1998.

Steele, D. P., and D. J. McEwen, Electron auroral excitation efficiencies and intensity ratios, *J. Geophys. Res.*, *95*, 10,321, 1990.

Tsyganenko, N. A., and D. P. Stern, Modeling the global magnetic field of the large-scale Birkeland current systems, *J. Geophys. Res.*, *101*, 27,187, 1996.

Weatherwax, A. T., H. B. Vo, T. J. Rosenberg, S. B. Mende, H. U. Frey, L. J. Lanzerotti, and C. G. MacLennan, A dayside ionospheric absorption perturbation in response to a large deformation of the magnetopause, *Geophys. Res. Lett.*, *26*, 517, 1999.

Yahnin, A. G., V. G. Vorobjev, T. Bosinger, R. Rasinkangas, D. G. Sibeck, and P. T. Newell, On the source region of traveling convection vortices, *Geophys. Res. Lett.*, *24*, 237, 1997.

Zesta, E., W. J. Hughes, M. J. Engebretson, T. J. Hughes, A. J. Lazarus, and K. I. Paularena, The November 9, 1993, traveling convection vortex event: A case study, *J. Geophys. Res.*, *104*, 28,041, 1999.

Zesta, E., W. J. Hughes, and M. J. Engebretson, A statistical study of traveling convection vortices using MACCS, *J. Geophys. Res.*, *107*, doi:10.1029/1999JA000386, in press, 2002.

Zhu, L., R. W. Schunk, and J. J. Sojka, Effects of magnetospheric precipitation and ionospheric conductivity on the ground magnetic signatures of traveling convection vortices, *J. Geophys. Res.*, *104*, 6773, 1999.

H. U. Frey, Space Sciences Laboratory, University of California, Berkeley, CA, USA.

D. L. Murr and W. J. Hughes, Center for Space Physics, Boston University, Boston, MA, USA.

A. S. Rodger, British Antarctic Survey, Cambridge, UK.

A. T. Weatherwax, Institute for Physical Science and Technology, University of Maryland, College Park, MD, USA.

E. Zesta, Department of Atmospheric Sciences, University of California Los Angeles, Los Angeles, CA, USA.